clean technologies

MDPI

Article

Thermal Investigation of a Turbocharger Using IR Thermography

Hamed Savaripour [1,2], Shahab Alaviyoun [3] and Marc A. Rosen [4,*]

[1] Department of Mechanical Engineering, Technical and Vocational University (TVU), Tehran 1435761137, Iran; hamed.basir89@gmail.com
[2] Design Department of Iran Khodro Powertrain Company, Tehran 1398813711, Iran
[3] Department of Mechanical Engineering, K.N. Toosi University of Technology, Tehran 1969764499, Iran; shalaviyoun@mail.kntu.ac.ir
[4] Faculty of Engineering and Applied Science, University of Ontario Institute of Technology, Oshawa, ON L1G 0C5, Canada
* Correspondence: marc.rosen@ontariotechu.ca

Abstract: An experimental thermal survey of a turbocharger was performed in an engine test cell using IR thermography. The emissivity coefficients of housings were specified using a furnace and camera. It was shown that the emissivity of the turbine, compressor, and bearing housings are 0.92, 0.65, and 0.74, respectively. In addition, thermocouples were mounted on the housing to validate the temperature of the thermal camera while running in an engine test cell. To compare the data of the thermocouple with data from the thermal camera, an image was taken from the sensor's location on the housing. The experimental results show that the temperature prediction of the thermal camera has less than 1 percent error. Steady-state tests at various working points and unsteady tests including warm-up and cool-down were performed. The measurements indicate that the turbine casing's maximum temperature is 839 °C. Furthermore, a thermal image of the bearing housing shows that the area's average temperature, which is close to the turbine housing, is 7 °C lower than the area close to the compressor housing. The temperature of the bearing housing near the turbine side should be higher; however, the effect of the water passing through the bearing housing decreases the temperature.

Keywords: experimental test results; gasoline engine; thermal camera; thermocouple; turbocharger

check for updates

Citation: Savaripour, H.; Alaviyoun, S.; Rosen, M.A. Thermal Investigation of a Turbocharger Using IR Thermography. *Clean Technol.* **2022**, *4*, 329–344. https://doi.org/10.3390/cleantechnol4020019

Academic Editors: Stanislaw Szwaja and Romualdas Juknelevičius

Received: 30 March 2022
Accepted: 26 April 2022
Published: 28 April 2022

Publisher's Note: MDPI stays neutral with regard to jurisdictional claims in published maps and institutional affiliations.

Copyright: © 2022 by the authors. Licensee MDPI, Basel, Switzerland. This article is an open access article distributed under the terms and conditions of the Creative Commons Attribution (CC BY) license (https://creativecommons.org/licenses/by/4.0/).

1. Introduction

In an internal combustion (IC) engine with a turbocharger, the energy available in the exhaust gases is used to rotate the turbine of the turbocharger [1]. The internal parts of the turbocharger are shown in Figure 1. The energy available in the exhaust gases is used to rotate the turbocharger turbine, which simultaneously drives the compressor to compress the intake air to the IC engine [2,3]. The compressor housing is usually made of aluminum. The air enters the center of the compressor housing, and the pressurized air exits radially [4]. The exhaust gases enter the turbine radially and leave it axially. The turbine housing, which is the hottest part of the turbocharger, is generally made of cast iron that can withstand hot gases up to 950 °C [5]. The bearing housing in a turbocharger is usually made of cast iron and is located between the turbine and compressor. The bearing housing includes bearings, seal rings, and gaskets. High-pressure oil enters the bearing housing and flows towards the bearings [6]. Finally, oil is drained from the bottom of the bearing housing. The oil film is located between the bearing and the bearing housing, and between the shaft and bearing. Oil is responsible for lubrication, cooling, and cleaning [7].

The turbochargers of diesel engines are generally cooled by the flow of oil and air passing around the bearing housing. However, in the turbocharger of a gasoline engine, the temperature of the exhaust gases is high, in some cases 1050 °C [8], so the bearing housing is cooled by oil and water [9]. Generally, gasoline turbochargers have a wastegate valve to

control the boost level produced in the intake manifold of a turbocharger by limiting the exhaust gas flow through the turbine wheel. The wastegate allows for a turbocharger with a smaller turbine and eliminates over-speed problems by bypassing a percentage of the exhaust gases from the turbine wheel. Using a smaller turbine reduces turbocharger lag and improves transient performance.

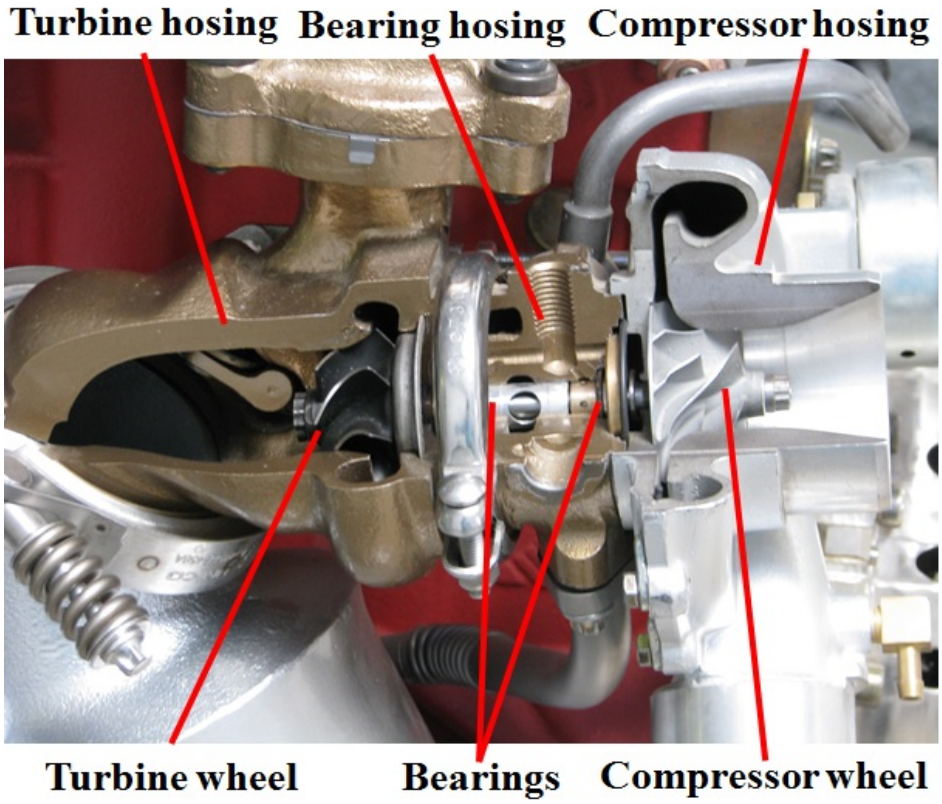


Figure 1. Turbocharger internal parts.

The fluid flow in the turbocharger is extremely complex, which has reverse flow and vorticities that occur in the housing. Therefore, computational methods were used to investigate the flow field in the turbocharger. For example, Benajes et al. [10] have simulated the flow field in the turbine housing of a turbocharger. In addition, Alaviyoun et al. [11] validated the full turbine model of a gasoline turbocharger using the pressure distribution and mass flow of gas. They showed that the gas velocity in the wastegate passage exceeds 500 m/s, demonstrating that the wastegate opening has a considerable effect on the temperature of the housing.

An object that has a temperature greater than zero Kelvin (−273 °C) emits infrared radiation. Depending on the object's geometry, the surface of the body, and its temperature, the infrared radiation waves are released at various intensities. The power of the infrared wave's emission is indicated with a coefficient called the emissivity factor. Thermography cameras measure the temperature. These cameras receive infrared waves according to their radiation intensity. The operator of the camera sets parameters such as ambient temperature, humidity, and the distance between camera and part.

Bohn et al. [12] measured the temperature distribution on the surfaces with a thermal camera. The results showed that the emissivity of the bearing housing was equal to the turbine housing, which may need more investigation. One of the reasons was the procedure that was used to find the emissivity of housings at 473 K, which is not the real working condition of the turbine housing. Based on these measurements, the temperature distribution on the surfaces was determined. The results include a parametric analysis

of 12 turbocharger operating conditions. The maximum temperature of the turbine shell increased almost linearly with turbine inlet temperature.

Baines et al. [13] performed experiments for three turbochargers equipped with thermocouples on the external and internal surfaces. They showed that thermal radiation had a significant role in external heat transfer. The highest external heat transfers occurred from the turbine to the environment and the bearing housing.

Romagnoli et al. [14,15] investigated the heat transfer of turbochargers on an engine under a constant speed and a constant load. According to the results, the temperature of the surface of the turbine near the exhaust manifold was 60 °C higher than the outer side of the housing. The main reason is the radiation from the exhaust manifold to the turbocharger.

Aghaali et al. [16,17] determined the amount of heat transfer in a turbocharger equipped with several temperature sensors. The results showed that the use of an external cooling fan significantly affects the energy balance of the turbocharger. In addition, the effect of cooling water is much higher than the external heat transfer at the bearing housing.

Jiaqiang et al. [18] investigated both numerically and experimentally the effect of boiling water on the heat transfer in the water pathways of a bearing housing in a gasoline turbocharger. They simulated a three-dimensional model of bearing housing and specified the effect of boiling on the amount of heat transfer.

Burke et al. [19] used 40 thermocouples to measure a wide range of fluid and solid temperatures of the turbocharger. The temperature was measured using sensors, each of 1.5 mm thickness. The response time for the thermocouple with a diameter of 1.5 mm is 10–30 s; however, the response time of a thermocouple with a smaller diameter increases the duration considerably.

Payri et al. [20] used 15 thermocouples to determine the convective heat transfer coefficient of the fluid passing through a turbocharger. To measure the wall temperatures, they used three thermocouples for each of the five axial cross-sections. The thermocouples have a 0.5 mm diameter with a measurement uncertainty of 1.5 K. An experimental investigation of steady-state and transient heat transfer was performed for a turbocharger test rig. Tadesse et al. [21], used six K-type thermocouples in tests to experimentally record the temperature distribution in a turbine housing. Additionally, an infrared camera was used to capture images during the transient test. However, each image includes a picture of the turbine and bearing housings, which leads to an error when the user wants to assign emissivity because the coefficients of these two parts are not the same. Basir et al. [22], using the thermal camera data, used the finite element method to find the temperature distribution in the turbocharger for all thicknesses. An acceptable level of agreement is observed by comparing the experimental data and the temperature distribution obtained from the simulation.

The literature review clarifies that most research uses thermocouples for the measurement of turbocharger wall temperature. Limited uses of infrared cameras are reported, which do not have high-quality images. Moreover, there are limited thermal images from turbocharger housings. The images captured in a turbocharger test rig can help attain an overview of the temperature distribution; however, it is not the actual engine operating condition of the part in the engine test cell. Therefore, the motivation for the current research is the implementation of an infrared camera to capture high-quality pictures that describe the temperature distribution of the turbine, compressor, and bearing housings in the engine test cell. The innovative aspect of the research is that it uses a new method to specify the emissivity factor of each housing (turbine, compressor, and bearing) in the working temperature. In this article, the radiation coefficient of the turbocharger is accurately determined using a furnace. The equipment needed for the test includes the infrared camera, the furnace, and the ambient temperature thermometer. To ensure the validity of the test and operating conditions of the furnace, the test was carried out in two types of furnaces, vertical and horizontal, with equivalent conditions. Due to the high accuracy of the test results for a vertical type of furnace, these results were used. The emissivity of

each housing is specified by the working temperature of the part. In addition, the effect of temperature on the emissivity of the turbine housing is investigated. Furthermore, in the experimental tests that were performed in the engine test cell, a set of thermocouples were installed on the turbocharger housings to measure the temperature of the housing surfaces in the real working condition of the turbocharger. The performance test of a gasoline engine with a turbocharger was performed at various engine operating points.

2. Radiation Coefficient of Turbocharger Parts

Objects emit electromagnetic waves that cover the continuous spectrum. The wavelength and amount of emitted power are dependent on the temperature of the object. Thermal imaging systems use radiation emitted from objects to capture images. Many photos with various radiation coefficients were captured and analyzed in this experiment.

2.1. Specifications of Furnaces (Vertical)

Table 1 shows the specifications of the vertical-type furnace that was used in the experiment.

Table 1. Specification of vertical furnace.

Characteristic	Value
Internal diameter of furnace (cm)	35
Height (cm)	50
Maximum power (kW)	14
Accuracy of temperature (°C)	±3
Maximum operating temperature (°C)	1200

2.2. Specifications of Thermal Camera

In this test, a thermal camera with Ti500 + THERMO HUNT model was used. Its specifications are listed in Table 2.

Table 2. Specifications of thermal camera.

Parameter	Volume
Temperature range	−20 to 1450 °C
Accuracy	±2 °C or ±2%
Filter ranges	Range 1 (−20 to 120 °C) Range 2 (0 to 500 °C) Range 3 (500 to 1500 °C)
Emissivity correction	Flexible 0.01 to 0.99 by 0.01 increments

2.3. Emissivity of the Compressor Housing

The temperature of the furnace was set to 195 °C. Other parameter such as ambient temperature and relative humidity were adjusted in the camera setting. The compressor housing was inserted into the furnace for 20 min until the temperature of the housing reached the furnace temperature. Photos were then taken, and three radiation coefficients were checked (0.55, 0.65, and 0.75), as shown in Figure 2. According to Figure 2, which shows the results of these images in the thermal software, because the temperature in the areas C1 and C2 are equal to the furnace temperature, it can be concluded that the emissivity of the compressor housing is 0.65.

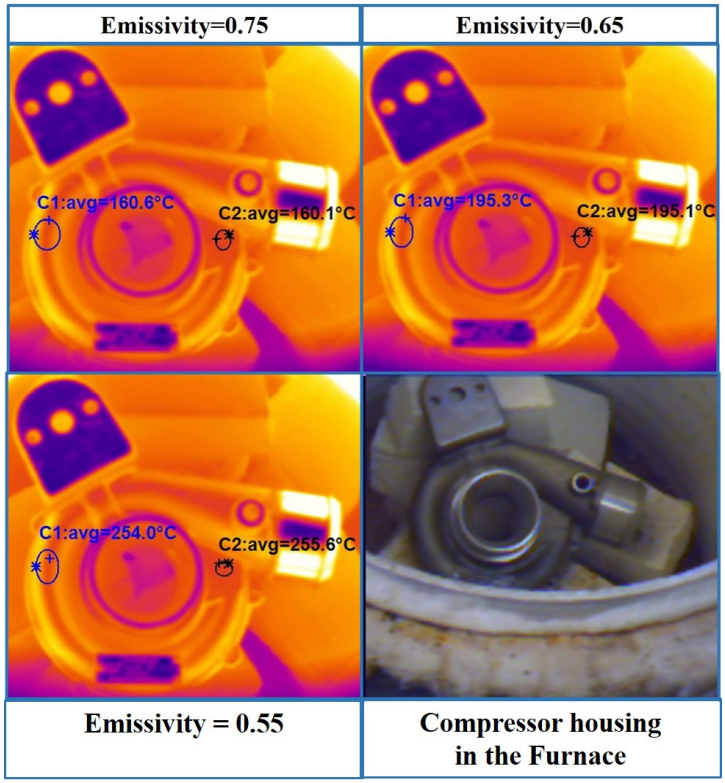


Figure 2. Thermal images of compressor housing for several emissivities, and compressor housing of the furnace (picture at lower right).

2.4. Emissivity of Bearing Housing

The bearing housing thermal image was taken with the thermal camera and is shown in Figure 3. It is seen that, at a furnace temperature of 160 °C, the correct emissivity of the bearing housing is 0.74. The emissivity of 0.74 for the bearing leads to an error of less than 1 °C in temperature measurements. The experiments were repeated three times to check the repeatability of the test.

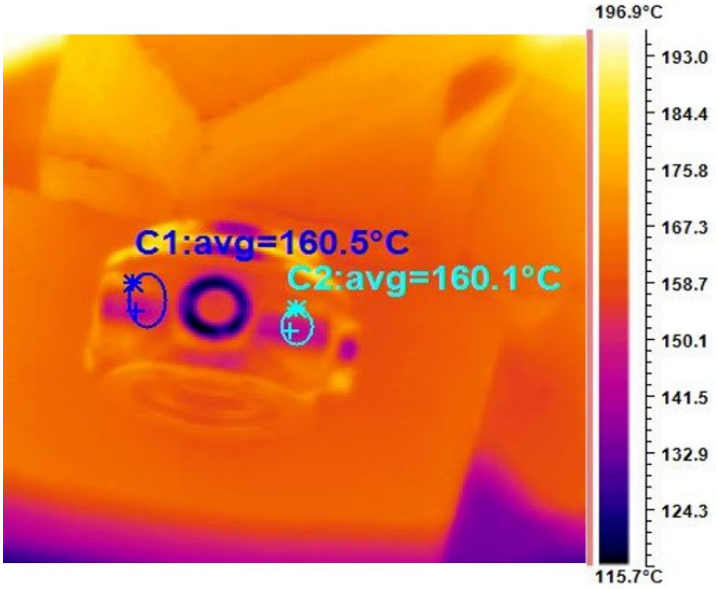


Figure 3. Bearing housing at 160 °C and emissivity of 0.74.

2.5. Emissivity of the Turbine Housing

The material of the turbine housing is D5S, which is cast iron with 30% nickel. It can resist a gas temperature up to 950 °C. The thermal image of the turbine housing that was taken at a temperature of 420 °C and an emissivity of 0.92 is shown in Figure 4. When the emissivity of the turbine in the camera is assigned a value of 0.92, the temperature of the image is equal to the temperature of the furnace.

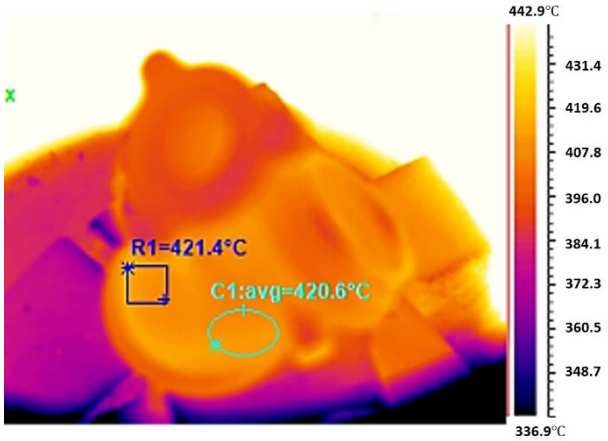


Figure 4. Turbine housing at 420 °C and an emissivity of 0.92.

The working temperature of the turbine housing is extremely broad, and it has a maximum surface temperature of 750 °C. Therefore, the emissivity of the housing was checked at three temperatures in the range of 420 to 750 °C. The results show that there is no significant change. However, as the temperature increases to 750 °C, the emissivity rises also slightly, from 0.92 to 0.94.

3. Experimental Test

In this experiment, thermocouples were placed at a depth of 1 mm from the turbocharger surface at different points around the compressor, bearing, and turbine housing. For instance, the location of one sensor on the turbine housing is shown in Figure 5. Sensors were installed around the housings' volute. It should be noted that one of the main constraints on adding points is the packaging limitation of the turbocharger on the engine. Figure 6 shows the location of some thermocouples on the turbocharger.



Figure 5. Location of a thermocouple on the turbocharger housing.

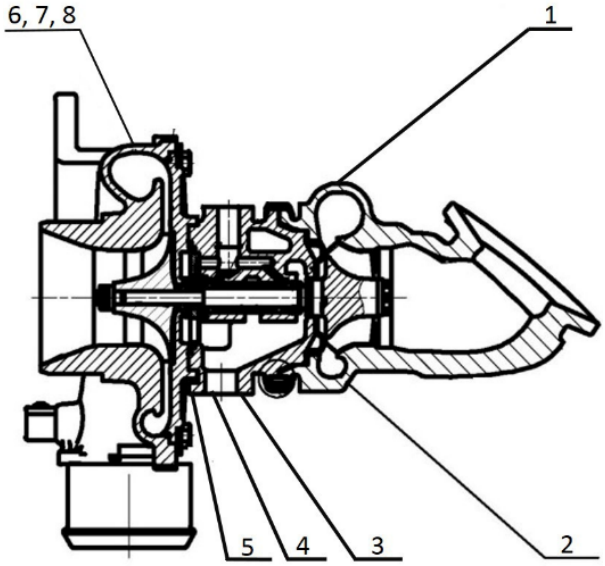


Figure 6. Schematic of installed thermocouples on the turbine housing.

The K-type thermocouple was used in this test. It has an operating range of −200 °C to +1200 °C and accuracy of ±2 °C. The experimental tests were performed in an engine test cell with a 1.7 L turbocharged engine. The specification of the engine and the turbocharger are provided in Table 3.

Table 3. Specifications of engine and turbocharger.

Parameter	Volume
No. of cylinders	4
Fuel type	Gasoline
Displacement (cc)	1700
Maximum power (kW)	110 (at 5500 rpm)
Maximum torque (Nm)	215 (at 2200–4800 rpm)
Maximum speed of the turbocharger	220,000 rpm
Compressor wheel diameter (mm)	51
Turbine wheel diameter (mm)	43
Turbocharger wastegate actuator	Pneumatic (pressurized)
Maximum temperature of turbine inlet gas (°C)	950
Material of turbine housing	GGG-NiSiCr 3552
Material of bearing housing	Cast iron (HT250)
Material of compressor housing	Aluminum alloy (ZL101)

At each working condition, thermal images were captured after the turbocharger temperature stabilized. The location of the camera inside the engine test cell is shown in Figure 7. The camera shows the turbine housing and the catalyst, which are the hot parts of the engine. The appropriate emissivity of the housing was applied. The temperature and humidity of the test cell were determined by the test cell sensors. Each test was repeated three times to ensure the repeatability of the measurements.

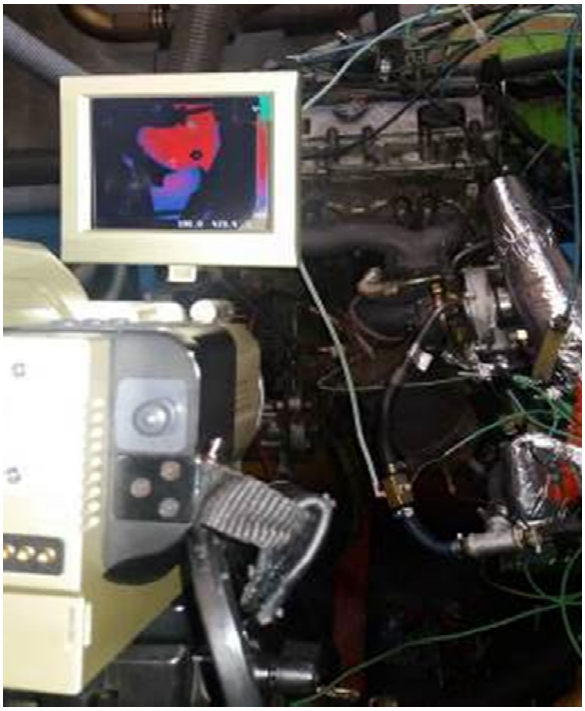


Figure 7. Engine test cell overview.

4. Test Results

4.1. Bearing Housing Test Results

The engine working point is 2500 rpm and the brake mean effective pressure (BMEP) is 5.2, which is a part-load condition. The bearing housing thermal images were captured when the thermal camera settings were applied (the emissivity of the bearing housing is adjusted to 0.74). Photos were analyzed using the software. The image of the thermal camera is shown in Figure 8, which is shown in the thermal analysis software. The section view of the bearing housing represents the water jacket path in the bearing housing.

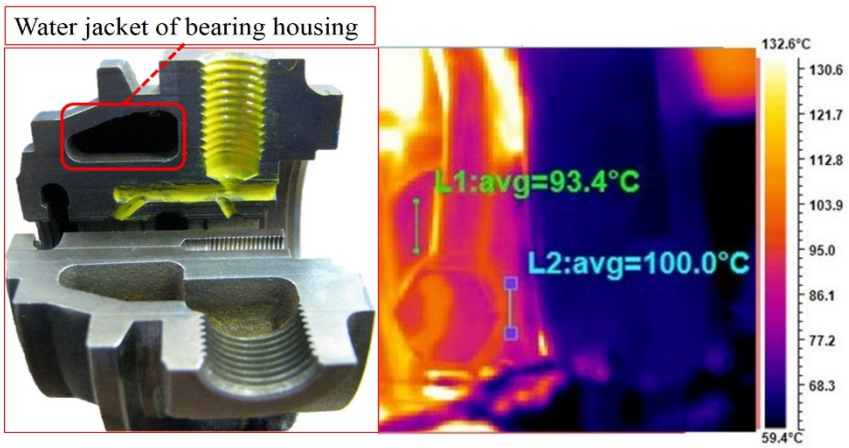


Figure 8. Turbocharger bearing system.

For the thermal analysis of different areas, there is a capability to draw lines on the object, and then the average temperature of the line could be determined. Moreover, the outputs of these lines are specified in the form of a temperature diagram. The software recognizes the beginning of the line from the left to the right and, for the vertical line, the software reads the line from the top to the bottom. The diagrams of lines L1 and L2, which are shown in Figure 8, are plotted by the thermal software in Figure 9.

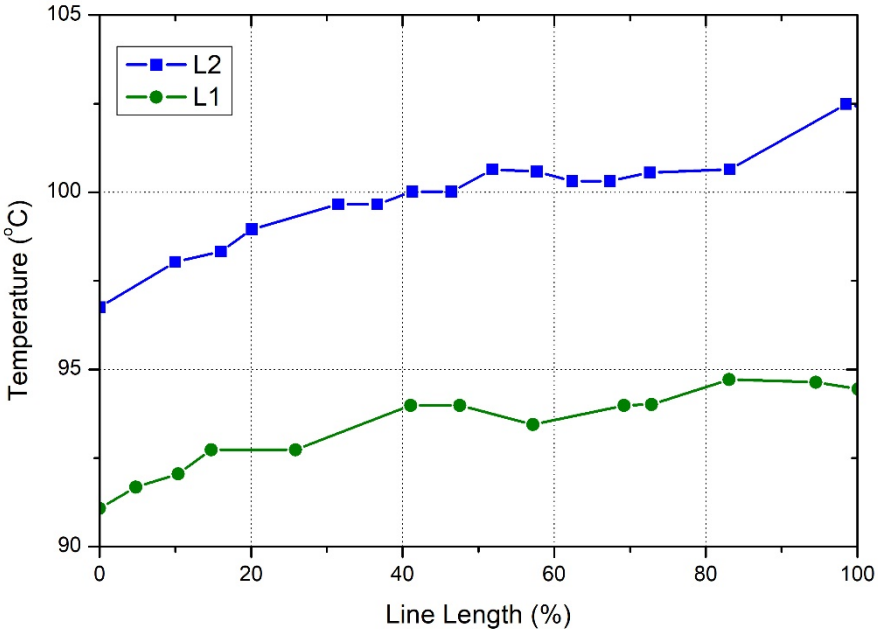


Figure 9. Bearings housing's heat transfer distribution diagram.

Engine coolant enters the bearing housing through the cooling path of the engine. As the water-cooling jacket is on the upper side of the bearing housing, the temperature of line L1 is lower than the temperature of line L2. Line L1 is selected on the surface-cooling path of the bearing housing. However, line L2 is far from the water-cooling path. The results show that the effect of cooling water is considerable in the bearing housing. Three temperature sensors were mounted at the bottom side of the bearing housing, which is shown in Figure 6. The measurement result shows that at a working point of 5500 rpm and full load condition of the engine, the maximum temperature of the housing is 155 °C. The maximum temperature is near the turbine side. The temperature of the bearing housing decreases as the distance from the turbine increases. The temperature difference along 3 cm of the bearing housing length is 33 °C. The measurement results show that, at this working point, the temperature of the compressor housing is 135.6 °C, which is higher than the bearing housing temperature at the compressor side. Therefore, it is concluded that, at the full load condition, heat is transferred from the compressor to the bearing housing. The bearing housing temperature at full load condition is provided in Table 4.

Table 4. Bearing housing temperature at full load condition.

Engine Speed (rpm)	Bearing Housing Temp. (Near Compressor, T5) (°C)	Bearing Housing Temp. (T4) (°C)	Bearing Housing Temp. (Near a Turbine, T3) (°C)
5500	122	124	155

4.2. Test Results for Turbine Housing

The engine working point is 2500 rpm with a BMEP of 4.9 bar, which represents the part-load condition. The thermal image of the turbine housing is shown in Figure 10.

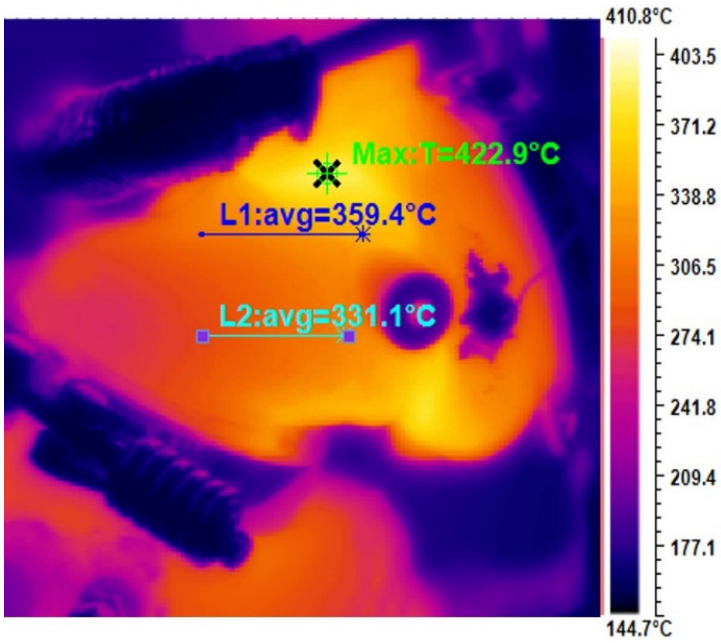


Figure 10. IR-image of the turbine housing.

A diagram of the heat transfer distribution through lines L1 and L2 on the surface of the turbine housing is shown in Figure 11. The temperature curves of lines L1 and L2 exhibit the same trend. It is shown that, as we get close to the turbine outlet flange, the temperature decreases. The temperatures of lines L1 and L2 increase from the left side to the right. For instance, the temperature difference between the two ends of line L2 is about 45 °C.

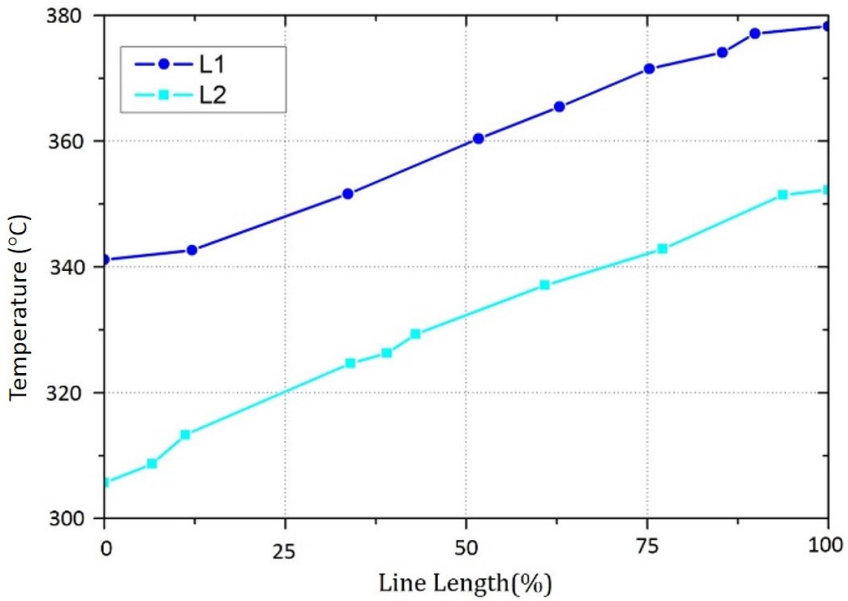


Figure 11. Turbine hosing's heat transfer distribution diagram.

In order to compare the temperatures from the thermocouples with the thermal camera results, images were captured from the locations at which the thermocouple is inserted. The dark area in the image (Figure 12) near line L1 is the glue that is used to fix the sensor on the surface of the turbine housing.

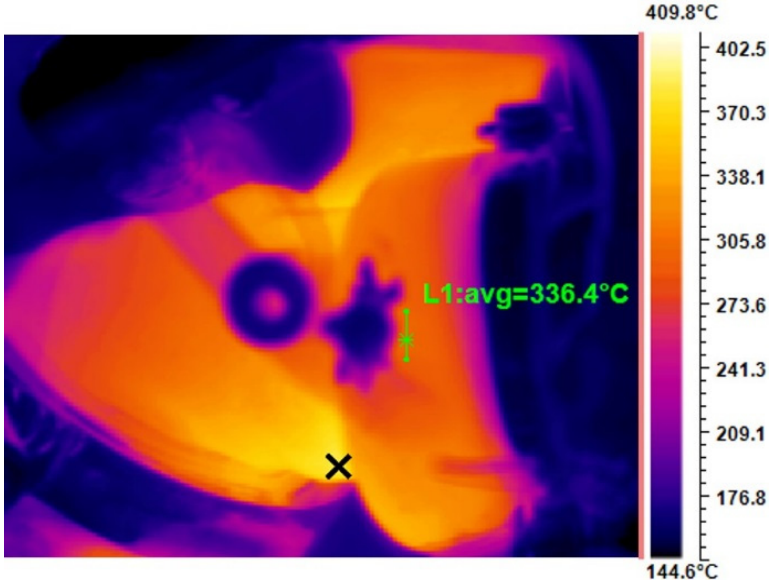


Figure 12. Position of thermocouple on the turbine housing.

The temperature distribution through line L1 is shown in Figure 13. It is seen that the temperature of the thermocouple installed on the turbine housing is 340 °C, while for the thermal camera images in Figure 14, the average temperature of line L1 near the sensor is 336.4 °C.

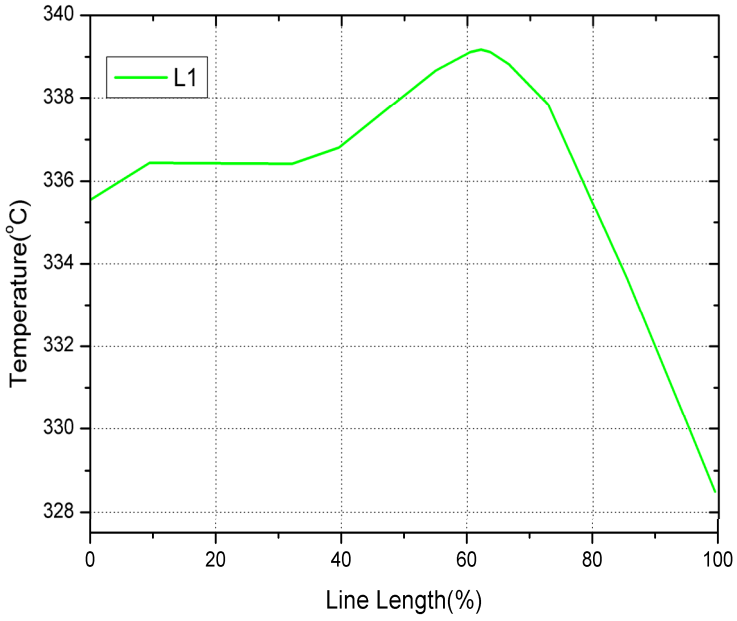


Figure 13. Spatial variation in turbine hosing heat transfer.

A comparison of the results of the thermal camera and the thermocouple indicates that the thermal camera error is less than 1 percent, which is acceptable.

The area on the turbine housing, which is machined, has a different emissivity factor than the bearing housing (Figure 14). Therefore, the temperature prediction of the machined surface is not accurate. However, this item does not affect the temperature measurement of the housing.

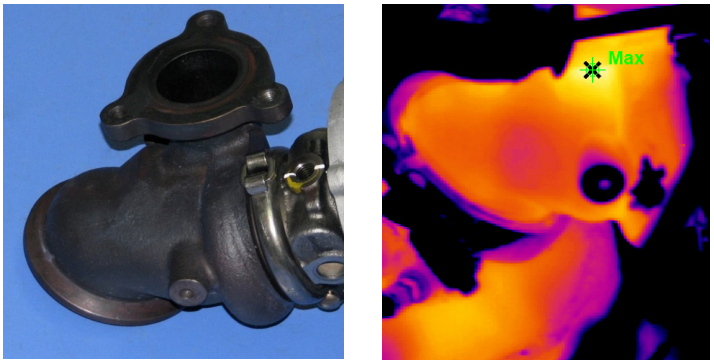


Figure 14. The area on the turbine housing that is machined.

4.3. Test Results for Compressor Housing

The compressor housing temperature at an engine speed of 5000 rpm and full load condition is investigated in Table 5. The temperatures of the compressor housing at three different points on the volute were measured, and it was observed that the temperature difference between point T8 and point T6 is 11.4 °C. The temperature of the housing increases as air passes through the volute and the maximum temperature occurs near the compressor outlet side. Heat is transferred from the compressed air, which is at a temperature of 143.9 °C, to the compressor housing.

Table 5. Compressor housing temperature.

Engine Speed (rpm)	Compressor Housing Temperatures (°C)		
	T6	T7	T8
5000	124.6	133.5	136

4.4. Cool-Down Test

In order to perform the turbine housing cool-down test, the thermal camera was located in the best position to capture photos in the engine test cell. At first, the engine was at an operating point of 5500 rpm and under full-load conditions. When the temperatures became stable, the test started, and the engine was turned off. Thermal images of the turbine housing were captured while the exact time of each image was recorded. The variations in the turbine housing cool-down temperatures with time (based on thermal camera images) are shown in Figure 15. The photos of the turbine housing during the cool-down test are shown at several time steps in Figure 16. Due to software limitations, it is not possible to have the same range of temperature for all four pictures in Figure 16. The results indicate that the position of the maximum temperature of the housing is at the same point after 210 s from the start of the test. The position is near the wastegate seating.

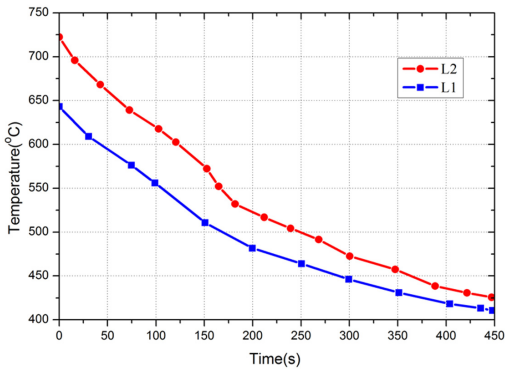


Figure 15. Variation in cool-down temperatures with time according to thermal camera images.

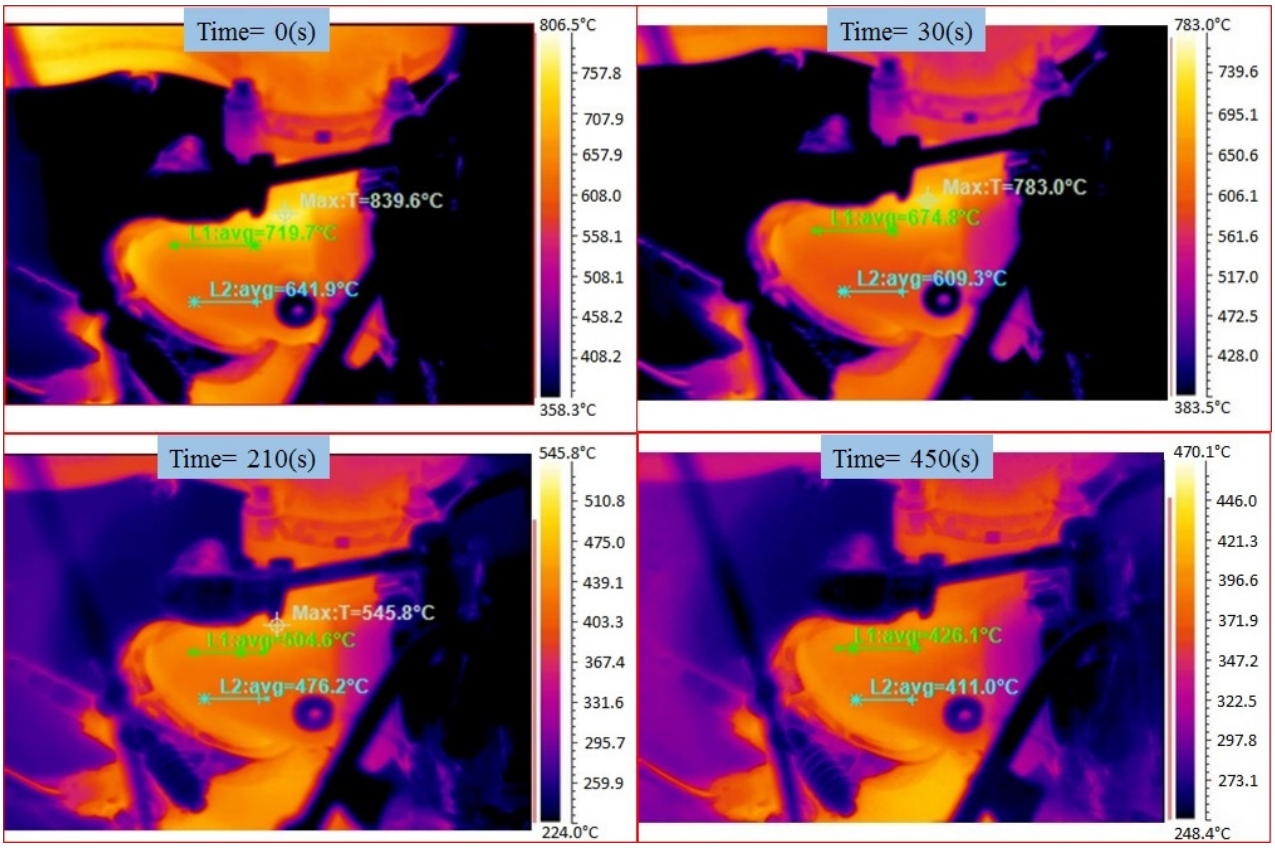


Figure 16. Turbine housing temperature distribution in cool-down mode.

4.5. Warm-Up Test

To perform the turbine housing warm-up test, the thermal camera was located in the best position to capture photos in the test room. Then, the engine was turned on and the working point moved directly to the engine speed of 2000 rpm and 28 N.m. The exact time of capturing images was recorded. The turbine temperature versus time variation for the warm-up test is shown in Figure 17. Figure 18 shows the thermal images of the turbine housing and temperature at two locations, four times.

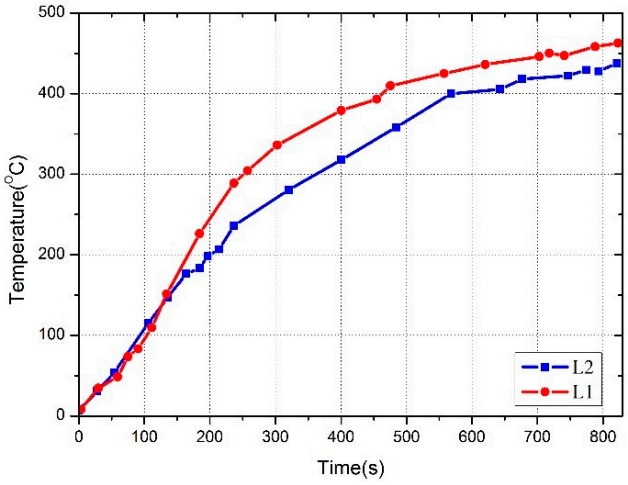


Figure 17. Variation in turbine housing warm-up temperature with time, based on data of the thermal camera.

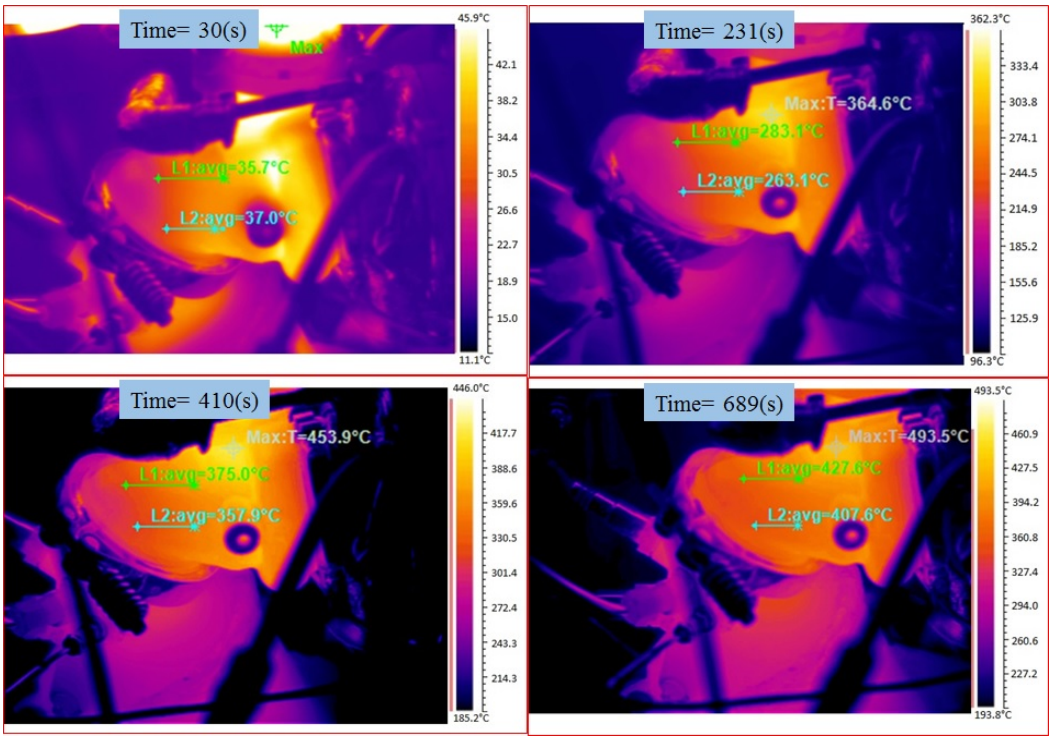


Figure 18. Heat transfer distribution of the turbine housing during a warm-up test.

5. Conclusions

An accurate method was used to predict the emissivity under high-temperature conditions. A performance test of a gasoline engine was performed at several engine operating points. Thermocouples were installed on the surface of the turbine, compressor, and bearing housing. During the engine tests, a series of steady-state tests were performed. In addition, unsteady tests, including warm-up and cool-down of the turbine housings, were investigated.

Based on the results at the first step of the cool-down test, the maximum temperature of the turbine housing is 839 °C, which occurs at an engine speed of 5500 rpm and full load conditions. The maximum temperature difference in the turbine housing surface is about 200 °C. The reason for such a high-temperature difference is radiation from the exhaust manifold, the wastegate opening, and the ventilation fan effect. Moreover, as the turbine housing becomes cooler during the cool-down test, the maximum temperature difference on the housing surface becomes smaller and reaches 70 °C after 210 s.

The maximum temperature of the housing is close to the wastegate seating position. Images of the cool-down test indicate that the location of the maximum temperature is constant until 210 s after the start of the test. The high temperature is near the wastegate area because some of the hot gases are bypassed directly through the wastegate without passing through the turbine blades. These hot gases cause an increase in body temperature near this area.

The maximum temperature of the compressor housing temperature at an engine speed of 5000 rpm and full load conditions is 136 °C. The results show that the maximum temperature of the compressor housing on the volute is near the outlet flange. Heat is transferred from the compressed air to the housing. The temperature difference between the compressed air and the housing is at least 13 °C.

The temperature of three sensors on the surface of the bearing housing was measured at an engine speed of 5500 rpm and full load conditions. The maximum temperature of the housing is near the turbine side which is 155 °C, and the minimum temperature is near the compressor side, at 122 °C. As the distance from the turbine increases, the temperature of the bearing housing decreases. The temperature of the compressor housing is 135.6 °C,

which is higher than the bearing housing temperature near the compressor. Therefore, it is concluded that, at the full load condition, heat is transferred from the compressor to the bearing housing. The temperature of the bearing housing is adjusted by the temperature of the water and oil passing through it. The high temperature of the turbine housing surface affects the bearing housing. However, the effect of cooling water decreases the temperature of the bearing housing near the turbine.

Author Contributions: All authors (H.S., S.A. and M.A.R.) have participated in conception, design, analysis, and interpretation of the data as well as the writing, drafting and revising the article. All authors have read and agreed to the published version of the manuscript.

Funding: This research received no external funding.

Data Availability Statement: Since the study is performed Thermal Investigation of a Turbocharger Using IR Thermography there is no need for ethical approval, however, all the tests are done in Irankhodro Powertrain Company (IPCo), in the Design Department, Engine Testing Lab, Automotive Laboratory, and Professional tests under the control of trained experts. Additionally, the paper main data is not published elsewhere.

Conflicts of Interest: The authors declare no conflict of interest.

References

1. Serrano, J.; Arnau, F.; Dolz, V.; Piqueras, P. Methodology for characterisation and simulation of turbocharged diesel engines combustion during transient operation. Part 1: Data acquisition and post-processing. *Appl. Therm. Eng.* **2009**, *29*, 142–149. [CrossRef]
2. Fu, J.; Shu, J.; Zhou, F.; Liu, J.; Xu, Z.; Zeng, D. Experimental investigation on the effects of compression ratio on in-cylinder combustion process and performance improvement of liquefied methane engine. *Appl. Therm. Eng.* **2017**, *113*, 1208–1218. [CrossRef]
3. Liu, J.; Fu, J.; Ren, C.; Wang, L.; Xu, Z.; Deng, B. Comparison and analysis of engine exhaust gas energy recovery potential through various bottom cycles. *Appl. Therm. Eng.* **2013**, *50*, 1219–1234. [CrossRef]
4. Galindo, J.; Tiseira, A.; Navarro, R.; Tarí, D.; Meano, C.M. Effect of the inlet geometry on performance, surge margin and noise emission of an automotive turbocharger compressor. *Appl. Therm. Eng.* **2017**, *110*, 875–882. [CrossRef]
5. Baines, N.C. *Fundamentals of Turbocharging*; Concepts NREC: White River Junction, VT, USA, 2005; ISBN 0-933283-14-8.
6. Chen, W.J. Rotordynamics and bearing design of turbochargers. *Mech. Syst. Signal Process.* **2012**, *29*, 77–89. [CrossRef]
7. Nguyen-Schäfer, H. *Rotordynamics of Automotive Turbochargers*; Springer: Berlin/Heidelberg, Germany, 2015.
8. Matsumoto, K.; Tojo, M.; Jinnai, Y.; Hayashi, N.; Ibaraki, S. Development of compact and high-performance turbocharger for 1050 °C exhaust gas. *Mitsubishi Heavy Ind. Tech. Rev.* **2008**, *45*, 1–5.
9. Zhao, J.; Ma, C.; Hu, L. Lightening structure optimization on turbine wheel of vehicular turbocharger. *Front. Energy Power Eng. China* **2008**, *2*, 422–426. [CrossRef]
10. Benajes, J.; Galindo, J.; Peña, P.F.; Navarro, R. Development of a segregated compressible flow solver for turbomachinery simulations. *J. Appl. Fluid Mech.* **2014**, *7*, 673–682.
11. Alaviyoun, S.; Ziabasharhagh, M.; Farajpoor, M. Experimental Investigation and Numerical Simulation of Gas Flow Through Wastegated Turbine of Gasoline Turbocharger. *J. Appl. Fluid Mech.* **2020**, *13*, 1835–1845.
12. Bohn, D.; Moritz, N.; Wolff, M. Conjugate flow and heat transfer investigation of a turbocharger: Part II—experimental results, in: ASME Turbo Expo 2003, collocated with the 2003 International Joint Power Generation Conference. *Am. Soc. Mech. Eng.* **2003**, *3*, 723–729. [CrossRef]
13. Baines, N.; Wygant, K.D.; Dris, A. The Analysis of Heat Transfer in Automotive Turbochargers. *J. Eng. Gas Turbines Power* **2010**, *132*, 042301. [CrossRef]
14. Romagnoli, A.; Martinez-Botas, R. Heat transfer analysis in a turbocharger turbine: An experimental and computational evaluation. *Appl. Therm. Eng.* **2012**, *38*, 58–77. [CrossRef]
15. Romagnoli, A.; Manivannan, A.; Rajoo, S.; Chiong, M.; Feneley, A.; Pesiridis, A.; Martinez-Botas, R. A review of heat transfer in turbochargers. *Renew. Sustain. Energy Rev.* **2017**, *79*, 1442–1460. [CrossRef]
16. Aghaali, H.; Ångström, H.-E. Turbocharged SI-engine simulation with cold and hot-measured turbocharger performance maps. In Proceedings of the ASME Turbo Expo 2012: Turbine Technical Conference and Exposition, Copenhagen, Denmark, 11–15 June 2012; pp. 671–679.
17. Aghaali, H.; Ångström, H.-E. A review of turbo compounding as a waste heat recovery system for internal combustion engines. *Renew. Sustain. Energy Rev.* **2015**, *49*, 813–824. [CrossRef]
18. Jiaqiang, E.; Zhang, Z.; Tu, Z.; Zuo, W.; Hu, W.; Han, D.; Jin, Y. Effect analysis on flow and boiling heat transfer performance of cooling water-jacket of bearing in the gasoline engine turbocharger. *Appl. Therm. Eng.* **2018**, *130*, 754–766. [CrossRef]

19. Burke, R.D. Analysis and Modeling of the Transient Thermal Behavior of Automotive Turbochargers. *J. Eng. Gas Turbines Power* **2014**, *136*, 101511. [CrossRef]
20. Payri, F.; Olmeda, P.; Arnau, F.J.; Dombrovsky, A.; Smith, L. External heat losses in small turbochargers: Model and experiments. *Energy* **2014**, *71*, 534–546. [CrossRef]
21. Tadesse, H.; Rakut, C.; Diefenthal, M.; Wirsum, M.; Heuer, T. Experimental Investigation of Steady State and Transient Heat Transfer in a Radial Turbine Wheel of a Turbocharger. In *Turbo Expo: Power for Land, Sea, and Air*; American Society of Mechanical Engineers: New York, NY, USA, 2015; Volume 56796, p. V008T23A015. [CrossRef]
22. Basir, H.; Gharehghani, A.; Ahmadi, A.; Mirsalim, S.M.A.; Rosen, M.A. Experimental and numerical investigation on the heat transfer of an automotive engine's turbocharger. *Proc. Inst. Mech. Eng. Part D J. Automob. Eng.* **2021**, *235*, 2124–2135. [CrossRef]